Monthly Notices
of the
ROYAL ASTRONOMICAL SOCIETY

MNRAS **504,** 4039–4053 (2021)
Advance Access publication 2021 April 21

doi:10.1093/mnras/stab1124

KIC 5950759: a high-amplitude δ Sct star with amplitude and frequency modulation near the terminal age main sequence

D. M. Bowman [1]★ J. Hermans,[1,2] J. Daszyńska-Daszkiewicz [3] D. L. Holdsworth [4] A. Tkachenko,[1] S. J. Murphy [5,6] B. Smalley [7] and D. W. Kurtz [4,8]

[1]*Institute of Astronomy, KU Leuven, Celestijnenlaan 200D, B-3001 Leuven, Belgium*
[2]*Centre for mathematical Plasma Astrophysics, KU Leuven, B-3001 Leuven, Belgium*
[3]*Astronomical Institute, University of Wrocław, ul. Kopernika 11, PL-51-622 Wrocław, Poland*
[4]*Jeremiah Horrocks Institute, University of Central Lancashire, Preston PR1 2HE, UK*
[5]*Sydney Institute for Astronomy (SIfA), School of Physics, University of Sydney, NSW 2006, Australia*
[6]*Stellar Astrophysics Centre, Department of Physics and Astronomy, Aarhus University, DK-8000 Aarhus C, Denmark*
[7]*Astrophysics Group, Lennard-Jones Laboratories, Keele University, Staffordshire ST5 5BG, UK*
[8]*Centre for Space Research, Physics Department, North-West University, Mahikeng 2745, South Africa*

Accepted 2021 April 16. Received 2021 April 13; in original form 2021 March 16

ABSTRACT

Among the intermediate mass pulsating stars known as δ Sct stars is a subset of high-amplitude and predominantly radial-mode pulsators known as high-amplitude δ Sct (HADS) stars. From more than 2000 δ Sct stars observed by the *Kepler* space mission, only two HADS stars were detected. We investigate the more perplexing of these two HADS stars, KIC 5950759. We study its variability using ground- and space-based photometry, determine its atmospheric parameters from spectroscopy and perform asteroseismic modelling to constrain its mass and evolutionary stage. From spectroscopy, we find that KIC 5950759 is a metal-poor star, which is in agreement with the inferred metallicity needed to reproduce its pulsation mode frequencies from non-adiabatic pulsation models. Furthermore, we combine ground-based WASP and *Kepler* space photometry, and measure a linear change in period of order $\dot{P}/P \simeq 10^{-6}$ yr^{-1} for both the fundamental and first overtone radial modes across a time base of several years, which is at least two orders of magnitude larger than predicted by evolution models, and is the largest measured period change in a δ Sct star to date. Our analysis indicates that KIC 5950759 is a metal-poor HADS star near the short-lived contraction phase and the terminal-age main sequence, with its sub-solar metallicity making it a candidate SX Phe star. KIC 5950759 is a unique object among the thousands of known δ Sct stars and warrants further study to ascertain why its pulsation modes are evolving remarkably faster than predicted by stellar evolution.

Key words: asteroseismology – stars: individual: KIC 5950759 – stars: oscillations – stars: variables: δ Scuti.

1 INTRODUCTION

One of the goals of astrophysics is to improve models of stellar evolution by using constraints from observations. Understanding the physical processes inside a star, such as convection, rotation, angular momentum transport, and mixing are of vital importance in improving stellar evolutionary models (Maeder & Meynet 2000; Maeder 2009). This is especially true for intermediate- and high-mass stars since they are born with a convective core, and the theoretical uncertainties associated with convection and mixing in the core-envelope boundary region strongly influence their post-main-sequence evolution (Kippenhahn, Weigert & Weiss 2012). Similarly, when such stars are close to depleting the hydrogen fuel in their cores, they enter an overall contraction phase to restore hydrostatic equilibrium, which results in a blue hook in the Hertzsprung–Russell (HR) diagram (Iben 1967). The location and morphology of this blue hook depends on the mass, metallicity, rotation rate, and the properties of convection within the star. One of the most promising techniques to mitigate these uncertainties and ultimately improve the predictive power of stellar evolution models is using observations of stellar pulsations. In this technique, known as asteroseismology, the resonant pulsation frequencies of a star are used to constrain its interior properties from a quantitative comparison to stellar models containing different input physics (Aerts, Christensen-Dalsgaard & Kurtz 2010; Aerts 2021).

Among intermediate mass Population I stars of spectral type A and F is a group of pulsating stars known as δ Sct stars, which have pulsation periods that range from ∼15 min to several hours (Breger 2000b; Aerts et al. 2010; Bowman & Kurtz 2018). They are located at the intersection of the main sequence and the classical instability strip in the HR diagram and have temperatures that range from approximately 7500 to 9500 K at the zero-age main sequence (ZAMS) and from approximately 6500 to 8500 K at the terminal-age main sequence (TAMS; Bowman & Kurtz 2018; Murphy et al. 2019). Thousands of δ Sct stars are known based on ground-based observations and surveys (Rodríguez, López-González & López de Coca 2000; Jayasinghe et al. 2020) and more recently space-based telescopes including *Kepler* (Borucki et al. 2010; Balona & Dziembowski 2011; Uytterhoeven et al. 2011) and *TESS* (Ricker et al.

★ E-mail: dominic.bowman@kuleuven.be

2015; Antoci et al. 2019). The parameter space covered by δ Sct stars in the HR diagram is of great importance for testing stellar evolution models. They cover the transition region from slowly rotating low-mass stars with radiative cores and thick convective envelopes ($M \lesssim 1.5$ M$_\odot$) to rapidly rotating intermediate mass stars with convective cores and predominantly radiative envelopes ($M \gtrsim 2.5$ M$_\odot$). This transition in stellar structure allows many different aspects of physics to be investigated, including pulsation, rotation, magnetic fields, and chemical peculiarities (see Murphy 2014 for a review).

Pulsations in δ Sct stars are typically excited by the opacity-driven heat engine κ mechanism operating in the He II ionization zone, which produces radial ($\ell = 0$) and non-radial ($\ell > 0$) pressure (p) modes with pulsation periods between ∼15 min and several hours (Breger 2000b; Pamyatnykh 2000). Many δ Sct stars are also observed to exhibit low-frequency variability caused by gravity (g) modes (see e.g. Balona & Dziembowski 2011), which are not predicted to be excited in early-A main-sequence stars without a significant modification to stellar opacity tables (Dupret et al. 2005; Balona, Daszyńska-Daszkiewicz & Pamyatnykh 2015). Recent work on the excitation of pulsations in these stars has revealed that turbulent pressure is also important for exciting higher radial order p modes (Antoci et al. 2014), and that the efficiency of mixing and the helium abundance in the near-surface layers of δ Sct stars plays an important role (Antoci et al. 2019; Murphy et al. 2020).

Within the pulsator group of the δ Sct stars, a small subset is observed to exhibit large pulsation amplitudes; these are known as high-amplitude δ Sct (HADS) stars (McNamara 1997, 2000b).[1] The HADS stars are in general slow rotators with projected surface rotational velocities of $v \sin i \lesssim 40$ km s^{-1}, which is in contrast to the moderate and high rotation rates of main-sequence A stars (Zorec & Royer 2012; Niemczura et al. 2015). In terms of their pulsation properties, HADS stars predominantly pulsate in the fundamental and/or first overtone radial p mode (Petersen & Christensen-Dalsgaard 1996; Breger 2000a; McNamara 2000b; Rodríguez et al. 2000; Derekas et al. 2009). The HADS stars were investigated by McNamara (2000b), who classified them as δ Sct stars with large peak-to-peak light amplitudes (typically exceeding 0.3 mag) and pulsation periods between 1 and 6 h. However, this historical classification is based only on inspection of the light curve, so it remains unclear why these stars are so rare and how they are distinct from their low amplitude δ Sct star cousins. For example, Lee et al. (2008) estimated that less than 1 per cent of pulsating A and F stars are HADS stars. Moreover, only two HADS stars were found within the sample of more than 10 000 A and F stars observed by the *Kepler* mission (Balona 2016; Bowman et al. 2016). Some HADS stars have been shown to be members of multiple systems based on their measured radial velocities (e.g. Derekas et al. 2009), although a complete census of binarity among HADS stars is lacking owing to their rarity.

In the literature, HADS stars have been sometimes thought of as transition objects between the main sequence δ Sct stars and the more-evolved classical (i.e. radial) pulsators, as they exhibit a tight period–luminosity (P–L) relationship similar to Cepheid variables (see e.g. Soszyński et al. 2008; Poleski et al. 2010). On the other hand, a P–L relationship for δ Sct stars investigated by Ziaali et al. (2019) contained considerably more scatter owing to these stars typically having both radial and non-radial modes with comparable amplitudes that exhibit long-term amplitude modulation (Bowman et al. 2016). Because of their rarity, there have only been a few detailed studies of HADS stars in the literature, which aimed to determine if these stars are distinct from δ Sct stars. For example, Petersen & Christensen-Dalsgaard (1996) claimed that HADS stars are able to pulsate at significantly higher amplitudes because they are in a post-main sequence stage of stellar evolution. On the other hand, Breger (2000a) conjectured that the slow rotation in these stars facilitates the high amplitude pulsations, which are not able to be excited in rapidly rotating δ Sct stars because of the deformation from spherical symmetry.

The Population II counterparts of δ Sct stars are known as SX Phe stars, named after the first such star to show high-amplitude radial pulsations (Frolov & Irkaev 1984), although such high-amplitude pulsation has been known since Goodricke (1783). SX Phe stars are also located within the classical instability strip in the HR diagram, have similar pulsation frequencies to δ Sct stars, and dominant radial pulsation modes with relatively large amplitudes like HADS stars (Balona & Nemec 2012). However, they sometimes have sub-solar metallicities and large spatial motions (McNamara 2000b; Nemec et al. 2017). Interestingly, SX Phe stars are known to exhibit period (i.e. pulsation frequency) changes when monitored over several years (Coates, Halprin & Thompson 1982; Thompson & Coates 1991; Rodríguez et al. 2007; Yang, Fu & Zha 2012; Murphy et al. 2013b), and yet these changes are sometimes observed as sudden jumps in period rather than smooth variation over time (e.g. Rodríguez et al. 1995). Therefore, it remains unclear if the period changes and associated amplitude modulation of pulsation modes are directly caused by stellar evolution. Recently, Daszyńska-Daszkiewicz et al. (2020) performed detailed seismic modelling of the prototype of this class, SX Phe, constrained its fundamental parameters and confirmed its post-main-sequence evolutionary phase thanks to high-precision photometry assembled by the *TESS* mission.

In this paper, we present the study of the pulsating star KIC 5950759, which is one of only two HADS stars observed by the *Kepler* space telescope during its nominal 4-yr mission. In Section 2, we use *Kepler* and Wide Angle Search for Planets (WASP) photometry to extract its pulsation mode frequencies and measure their long-term variability. In Section 3, we present our spectroscopic analysis of KIC 5950759, and in Section 4 we use *Gaia* parallaxes to calculate its luminosity. We perform forward asteroseismic modelling of KIC 5950759 in Section 5, and we conclude in Section 6.

2 PHOTOMETRY

KIC 5950759 was first identified as a variable star with a dominant period of 0.0703176 d by Pigulski et al. (2009) using ASAS data. Later, it was identified as one of only two HADS stars in the nominal field of view of the *Kepler* mission (Balona 2016; Bowman et al. 2016), which satisfied the criterion of having large peak-to-peak light amplitude variations typical of such stars (McNamara 2000b). The parameters of KIC 5950759 from the *Kepler* Input Catalogue (KIC; Brown et al. 2011) and the revised values from Huber et al. (2014), which are similar to the updated values of Mathur et al. (2017), are provided in Table 1.

2.1 *Kepler* photometry

In this work, light curves from the multi-scale Maximum A Priori Pre-Search Data Conditioning (msMAP PDC) pipeline developed by the *Kepler* Science Office (Smith et al. 2012; Stumpe et al. 2012)

[1] McNamara (1997) credit the classification of HADS stars as a distinct group of pulsators to an unpublished Harvard university dissertation of H. Smith in 1955.

Table 1. Stellar parameters of KIC 5950759 from photometric catalogues and spectroscopy from this work (see text for details), including the effective temperature ($T_{\rm eff}$), surface gravity (log g), and metallicity ([M/H]).

$T_{\rm eff}$ (K)	log g	[M/H] (dex)	Reference
7840 ± 300	4.03 ± 0.25	−0.07 ± 0.25	Brown et al. (2011)
8070 ± 280	4.03 ± 0.40	−0.07 ± 0.30	Huber et al. (2014)
7340 ± 220	2.9 ± 1.3	−1.18 ± 0.30	this work
7470 ± 255	3.6 ± 1.2	−0.65 ± 0.45	this work

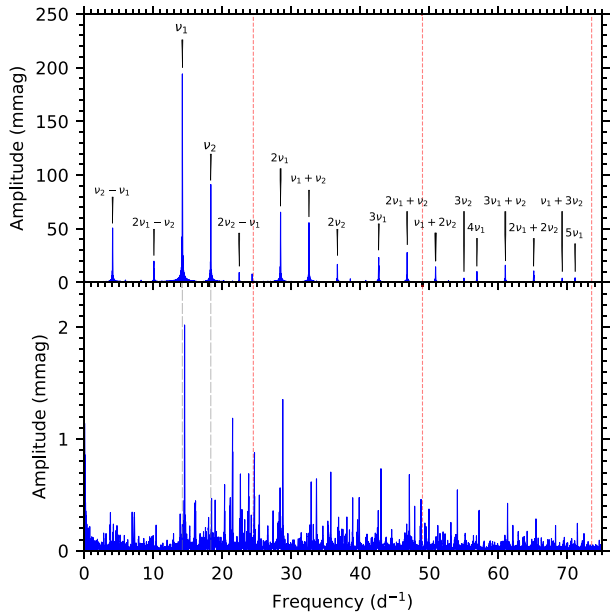

Figure 1. Top panel: the amplitude spectrum calculated from the one month of SC *Kepler* data for KIC 5950759, in which the two dominant pulsation modes, ν_1 and ν_2, and their high-amplitude combination frequencies are labelled. Bottom panel: the residual amplitude spectrum of the same SC *Kepler* data after ν_1 and ν_2 and all their significant combination frequencies have been removed by pre-whitening. The long-dashed grey lines denote the location of ν_1 and ν_2 in the bottom panel, and the short-dashed red lines indicate integer multiples of the *Kepler* LC Nyquist frequency to demonstrate that considerable variance remains beyond the *Kepler* LC Nyquist frequency.

are used, which are publicly available from the Mikulski Archive for Space Telescopes (MAST).[2] KIC 5950759 was observed between Q1 and Q17 of the nominal *Kepler* mission in its long cadence (LC; 29.5 min) mode, for a total of 1460 d. It was also observed in the first month of Q4 in short cadence (SC; 59 s) mode for a total of 31.1 d. The effective Nyquist frequencies of the LC and SC data are 24.47 and 727.35 d^{-1}, respectively. The *Kepler* light curves were converted into stellar magnitudes and long-period instrumental systematics were removed by means of subtracting a low-order polynomial from each LC data quarter.

From the LC and SC light curves amplitude spectra were calculated by means of a discrete Fourier transform (Kurtz 1985). The amplitude spectrum of the single month of SC *Kepler* data is shown in the top panel of Fig. 1, in which the two high-amplitude pulsation modes, ν_1 and ν_2, and their dominant combination frequencies are labelled. The two high-amplitude modes have a period (and

[2]http://archive.stsci.edu/kepler/

Table 2. Frequency, amplitude, and phase of the two dominant pulsation modes, ν_1 and ν_2, in KIC 5950759, which were obtained using a non-linear least-squares fit to the 4-yr LC *Kepler* light curve, and the 31-d SC light curve. Pulsation phases were calculated with respect to the time zero-point t_0 = 2455688.770 BJD.

		Frequency (d^{-1})	Amplitude (mmag)	Phase (rad)
LC	ν_1	14.2213938 ± 0.0000009	167.7 ± 0.3	1.685 ± 0.002
	ν_2	18.3372939 ± 0.0000015	74.1 ± 0.3	1.178 ± 0.004
SC	ν_1	14.22137 ± 0.00005	194.1 ± 0.5	1.6 ± 0.1
	ν_2	18.33725 ± 0.00010	91.2 ± 0.5	1.0 ± 0.3

frequency) ratio of 0.77554 identifying them as the fundamental and first overtone radial modes (Breger 2000b). In δ Sct stars with such high-amplitude (radial) pulsation modes, it is typical to observe many high-order harmonics and combination frequencies – i.e. frequencies that can be identified using $n\nu_1 \pm m\nu_2$, in which n and m are integers (Pápics 2012; Kurtz et al. 2015; Balona 2016). The physical causes of combination frequencies include the stellar medium not responding linearly to a pulsation wave, or that the flux variability caused by waves is not a linear transformation of the temperature variability (see e.g. Brickhill 1992). These phenomena are generally grouped together into what is called a non-linear distortion model (e.g. Degroote et al. 2009; Bowman 2016). On the other hand, some combination frequencies represent resonantly excited pulsation modes that are the result of direct mode coupling (see e.g. Breger & Montgomery 2014; Bowman et al. 2016).

A detailed frequency analysis of both the LC and SC *Kepler* data of KIC 5950759 was originally performed by Bowman (2017), which focused on the two radial modes and their combination frequencies. Since the much longer 4-yr LC *Kepler* data set provides significantly better frequency resolution and precision, Bowman (2017) extracted and optimized the parameters of the two dominant pulsation modes, ν_1 and ν_2, using a multifrequency non-linear least-squares fit to the LC *Kepler* light curve with the equation:

$$\Delta m = \sum_i A_i \cos\left(2\pi\nu_i\left(t - t_0\right) + \phi_i\right), \quad (1)$$

where A_i is the amplitude, ν_i is the frequency, ϕ_i is the phase, t is the time with respect to the zero-point t_0 = 2455688.770 BJD (i.e. the midpoint of the 4-yr *Kepler* light curve) for i frequencies. The resultant parameters for ν_1 and ν_2 are provided in Table 2.

Bowman (2017) also performed a similar optimization of the two dominant pulsation modes using equation (1) and a non-linear least-squares fit to the SC *Kepler* data of KIC 5950759. Since the SC *Kepler* data have a much higher Nyquist frequency, Bowman (2017) calculated the expected frequencies of combination frequencies of ν_1 and ν_2 up to order of 20 (i.e. $n\nu_1 \pm m\nu_2$, where $n, m \in [0, 20]$), and optimized their amplitudes and phases using a multifrequency linear least-squares fit, and subtracted them from the SC *Kepler* light curve to reveal any additional independent pulsation modes. Such high harmonic and combination orders are necessary for KIC 5950759 given the high amplitudes of the parent modes (i.e. ν_1 and ν_2) and the pristine quality of *Kepler* data. For example, the twentieth harmonic of ν_1 (i.e. $20\nu_1$) is significant in the SC data of KIC 5950759 with an amplitude of approximately 10 μmag. By using the approach of calculating the expected combination frequencies, any variance coinciding with the expected frequencies of combinations is removed from the light curve by means of subtracting the multifrequency linear least-squares fit solution. The amplitude spectra of the SC

Kepler light curve up to 75 d^{-1} both before and after removing ν_1, ν_2 and all their combination frequencies are shown in the top and bottom panels of Fig. 1, respectively, which clearly demonstrates additional variance in KIC 5950759.

Yang et al. (2018) later performed an independent frequency analysis of the available *Kepler* data of KIC 5950759. They confirmed the previous characterization of ν_1 and ν_2 as radial modes and investigated a detected weak modulation effect present in KIC 5950759, which resulted in equally spaced frequency multiplets around the dominant pulsation modes. The separation between the frequencies of these multiplets, 0.31923 d^{-1}, was also detected as a significant frequency in the amplitude spectrum. Yang et al. (2018) concluded that these multiplets could be caused by amplitude modulation of the radial modes from the rotation of the star.[3] Such a modulation mechanism acting on radial modes has been found in some δ Sct stars (e.g. Breger et al. 2011), but its physical cause remains difficult to interpret. The inferred rotation frequency from the multiplets, 0.31925 d^{-1}, would indicate a slow rotation rate, which is expected for HADS stars. For a discussion of this modulation effect, we refer the reader to Yang et al. (2018).

More recently, Hermans (2019) re-visited the frequency analysis of KIC 5950759 for the specific purpose of identifying additional non-radial modes. The same LC and SC light curves studied by Bowman (2017) were analysed by Hermans (2019) for consistency and comparison purposes. The LC and SC data were subjected to iterative pre-whitening, and modelled as a linear superposition of modes, as is typical for pulsating stars (see e.g. Degroote et al. 2009; Pápics et al. 2012; Van Reeth et al. 2015; Antoci et al. 2019). During each iteration, the frequency of the highest amplitude peak is determined, optimized to the light curve using equation (1), which yields the optimized frequency, amplitude, and phase. The resulting cosinusoid model is then subtracted from the light curve and the residual time series is used as input in the next iteration. The standard stop criterion of an amplitude signal-to-noise (S/N) criterion of four (Breger et al. 1993) was used by Hermans (2019) to extract all significant frequencies, in which the noise was calculated as the median amplitude in a window of 1 d^{-1} centred on the extracted frequency at each iteration.

A total of 150 significant frequencies were identified in the LC *Kepler* data in the frequency interval of $0 \leq \nu \leq 120$ d^{-1}, and 106 significant frequencies in the SC *Kepler* data of KIC 5950759 in the frequency interval $0 \leq \nu \leq 200$ d^{-1} by Hermans (2019). Although pulsation modes with frequencies above 60 d^{-1} are rare in δ Sct stars (Bowman & Kurtz 2018), the large frequency range was chosen to ensure that high-frequency non-radial modes were not excluded. From these lists of extracted significant frequencies, spurious frequencies were filtered using the resolution criterion proposed by Loumos & Deeming (1978), such that the minimal frequency separation between independent close frequencies, ν_x and ν_y, satisfied

$$|\nu_x - \nu_y| \geq \frac{1.5}{\Delta T}, \tag{2}$$

where ΔT is the length of the data set. The highest amplitude peak was kept during the filtering for spurious frequencies. Combination frequencies were identified by searching for linear sum and difference frequencies, $n\nu_i \pm m\nu_j$, with the Loumos & Deeming (1978) criterion as a tolerance and assuming that the highest-amplitude peaks within a combination family are the real pulsation mode frequencies (Kurtz et al. 2015). Although the Loumos & Deeming (1978) criterion is not a formal frequency precision (see e.g. Lares-Martiz, Garrido & Pascual-Granado 2020), it does act as a conservative metric for identifying combination frequencies given the added uncertainties introduced in the form of spurious frequencies from an imperfect linear least-squares pre-whitening methodology (see e.g. Degroote et al. 2009; Pápics et al. 2012; Van Reeth et al. 2015; Antoci et al. 2019). Finally, Nyquist alias frequencies were identified by cross-matching the resultant list of filtered frequencies in the LC and SC analysis, and by applying the super-Nyquist technique (Murphy, Shibahashi & Kurtz 2013a) to the LC *Kepler* data.

In total, 12 and 13 independent pulsation mode frequencies (i.e. those that cannot be explained as spurious close frequencies, combination frequencies, or Nyquist aliases) were identified from the LC and SC data in addition to ν_1 and ν_2 (cf. Table 2), which are given in Tables A1 and A2, respectively. Therefore, in addition to the two high-amplitude radial pulsation modes, ν_1 and ν_2, KIC 5950759 reveals multiple additional non-radial pulsation modes. Unfortunately, mode identification is not possible for these non-radial modes owing to their lack of regularity in the extracted frequencies. We also note that the same frequency multiplets found by Yang et al. (2018) centred on the radial mode frequencies are present in both LC and SC data, but have much lower S/N values in the SC data. For example, the modulation frequency, 0.31925 ± 0.00004 d^{-1}, is only significant in the LC data because of the lower local noise level.

2.2 WASP photometry

Given the extremely high-frequency precision provided by its high-amplitude radial modes using *Kepler* data, Bowman (2016) identified KIC 5950759 as an excellent candidate to probe pulsation period changes. Moreover, ground-based photometric surveys prior to and during the *Kepler* mission have also been able to monitor its high-amplitude pulsation modes. A naturally complementary photometric survey to our analysis of the *Kepler* light curve of KIC 5950759 is the WASP project, which was a wide-field and ground-based photometric survey that aimed to find transiting exoplanets (Pollacco et al. 2006; Butters et al. 2010). The project had two observing sites, one at the Observatorio del Roque de los Muchachos on La Palma and the other at the Sutherland Station of the South African Astronomical Observatory. The pixel size of each instrument is approximately 14 arcsec with observations made using broad-band filters of 400–700 nm, which are slightly more sensitive to bluer wavelengths compared to the *Kepler* passband. WASP data are corrected for extinction, the colour-response of the instrument, the zero-point, and instrumental systematics using the SYSREM algorithm (Tamuz, Mazeh & Zucker 2005). The observing strategy of WASP provided two consecutive 30-s exposures at a given pointing, before moving to the next available field. Each field was typically revisited every 10 min on a given night, which produces a high effective Nyquist frequency (Holdsworth 2015).

The WASP survey observed KIC 5950759 for three seasons in 2007, 2009, and 2010, with light curves spanning 65.8, 127.9, and 122.9 d, respectively. Although the photometric precision and number of data points are not as high in each WASP light curve compared to the LC *Kepler* data, the high-amplitude pulsation modes in KIC 5950759 are easily detectable. Moreover, during 2009 and 2010, data collection by both WASP and *Kepler* were concurrent. This has great advantages and allows us to use the WASP data

[3]To be clear, this does not mean rotational splitting of radial modes, since this is not possible, but rather means that the pulsation amplitudes of the radial modes varies during the rotation phase causing equally spaced multiplets in the amplitude spectrum.

to probe the variability in KIC 5950759 prior to the launch of the *Kepler* space telescope, as previously demonstrated using the δ Sct star KIC 7106205 by Bowman, Holdsworth & Kurtz (2015). To compare simultaneous WASP and LC *Kepler* observations of KIC 5950759 in 2009 and 2010, the *Kepler* data were truncated to have the same length as the individual WASP seasons. Also, the time stamps of the WASP data, which were originally in HJD (UTC), were converted to BJD (TDB) using the PYTHON module ASTROPY (Astropy Collaboration 2013, 2018) to be fully consistent in both time-scale and format with the *Kepler* data. An example of the concurrent LC *Kepler* and WASP light curves for KIC 5950759 in 2010 are shown in the top panel of Fig. 2. The lower panels in Fig. 2 show the amplitude spectra of the WASP data (right-hand panels) and the truncated *Kepler* data (left-hand panels).

Because of the discrete and finite sampling of an instrument's integration time, a star's pulsation modes are suppressed in amplitude because of an effect known as apodization or the amplitude suppression function (Bowman et al. 2015). The observed pulsation amplitudes can be corrected using

$$A = A_0 \,\mathrm{sinc}\left(\frac{\pi}{n}\right) = A_0 \,\mathrm{sinc}\left(\frac{\pi\,\nu}{\nu_{\mathrm{samp}}}\right), \tag{3}$$

where A and A_0 are the observed and intrinsic pulsation mode amplitudes, respectively, n is the number of data points per pulsation cycle, ν is the pulsation mode frequency and ν_{samp} is the instrument's sampling frequency (Murphy 2014; Bowman 2017).

A second correction arising from the difference in instrument passband is also needed, since the WASP passband is slightly more sensitive to bluer wavelengths compared to *Kepler*, such that observed pulsation amplitudes of A and F stars are (slightly) larger when observed at bluer wavelengths. We use the resultant value for this passband correction from Bowman et al. (2015), who estimated this correction factor to be 7.6 per cent for the late-A star KIC 7106205 – i.e. pulsation mode amplitudes are 7.6 per cent smaller in *Kepler* observations compared to WASP observations because of the difference in effective wavelength range of their passbands.[4]

Thus we corrected the WASP and truncated *Kepler* data obtained in 2009 and 2010 for their respective instrument's integration time, and then transformed the WASP pulsation mode amplitudes into the *Kepler* passband using the passband correction factor from Bowman et al. (2015). The remaining difference between the pulsation mode amplitudes observed by WASP and *Kepler* in 2009 and 2010 is because of flux dilution from nearby and background stars within the larger WASP aperture (Bowman et al. 2015). A ratio of the respectively corrected WASP and *Kepler* mode amplitudes in 2009 and 2010 reveals an average dilution factor of 2.2 ± 0.1 – i.e. the integration time and passband corrected WASP amplitudes are approximately 45 per cent those of the *Kepler* amplitudes. Of the integration time, passband and dilution correction factors, the latter is certainly the largest effect and the largest source of uncertainty in this analysis. This is already evident in the non-corrected amplitude spectra shown in Fig. 2.

After the integration time, passband and dilution correction factors were determined and applied to the 2009 and 2010 WASP data, they were also applied to the 2007 WASP data to estimate the amplitude of the fundamental and first overtone radial modes in KIC 5950759.

[4]More generally, this factor depends on the effective temperature of the star and the pulsation mode geometry, but for A and F stars the difference between *Kepler* and WASP amplitudes is of the order of 10 per cent.

We provide the results for the corrected WASP amplitudes of ν_1 and ν_2 in the top-left and top-right panels of Fig. 3, respectively. We also divided the 4-yr *Kepler* data into bins of 150 d with 100-d overlap, following the technique employed by Bowman et al. (2016), and show the amplitude and phase as a function of fixed frequency (cf. Table 2) in Fig. 3. The quasi-sinusoidal variability in the pulsation amplitudes in the LC *Kepler* data has a period equal to that of the *Kepler* orbital period, and is caused by a changing signal-to-background flux ratio caused by the rotation of the spacecraft every 90 d. Thus, it is of instrumental and not astrophysical origin, although the amplitude is arguably constant within 2σ regardless. Despite the relatively large amplitude uncertainties associated with the WASP data in 2007, we conclude that there is tentative evidence for a growing amplitude in the fundamental and first overtone radial modes in KIC 5950759 prior to the start of the *Kepler* observations.

2.3 Period changes

During the main sequence and post-main-sequence phases of stellar evolution, an intermediate mass star experiences an increase in radius, which increases the size of the acoustic cavity of its radial pulsation modes, hence the periods of radial modes increase with age. On the other hand, the relatively short-lived overall contraction phase near the TAMS, which results in a 'blue hook' in the HR diagram for intermediate mass stars (Iben 1967; Kippenhahn et al. 2012), is a phase of evolution in which the stellar radius decreases such that the periods of radial modes are expected to decrease. Consequently, the rate of change in the periods of radial modes theoretically allow stellar evolution to be measured (Walraven, Walraven & Balona 1992; Breger & Pamyatnykh 1998).

Period changes in pulsation modes have been historically studied by means of the O − C technique (Percy, Matthews & Wade 1980; Sterken 2005). Based on the work of Breger & Pamyatnykh (1998), period changes in pulsation modes can be determined from

$$\mathrm{O-C} = \frac{1}{2}\left(\frac{1}{P}\,\frac{\mathrm{d}P}{\mathrm{d}t}\right)t^2 = \frac{1}{2}\left(\frac{\dot{P}}{P}\right)t^2, \tag{4}$$

where O − C is the difference between the observed and calculated times of maxima in days, t is the time span of the observations in days, and P is the period of the signal in days, such that to convert the period change into its conventional units of yr^{-1} one uses the number of days in a year (i.e. 365.2422). Thus, equation (4) dictates that a linearly changing period produces a quadratic change in O − C (Percy et al. 1980; Breger & Pamyatnykh 1998; Sterken 2005).

In addition to studying the amplitude modulation of pulsation modes in KIC 5950759, the concurrent WASP and *Kepler* observations in 2009 and 2010 allow us the unique opportunity to probe its phase (i.e. frequency) modulation. Using the technique employed by Bowman et al. (2016), we calculate the pulsation phase using a linear least-squares fit to each of the 150-d bins of LC *Kepler* data, which is shown in the middle row of Fig. 3. Furthermore, to include the 2007 WASP data, as before we use the truncated 2009 and 2010 overlapping *Kepler* data to compare the pulsation phase during the concurrent 2009 and 2010 WASP seasons. Since we are assuming and fixing the pre-optimized pulsation mode frequencies of ν_1 and ν_2 (cf. Table 2), we perform an independent linear least-squares fit to each of the WASP and truncated *Kepler* data in 2009 and 2010. We compare the corresponding pulsation phases and find a constant phase offset of 0.54 ± 0.01 rad between the 2009 WASP and truncated 2009 *Kepler* data (and the same value between the 2010 WASP and truncated 2010 *Kepler* data). Such a phase offset

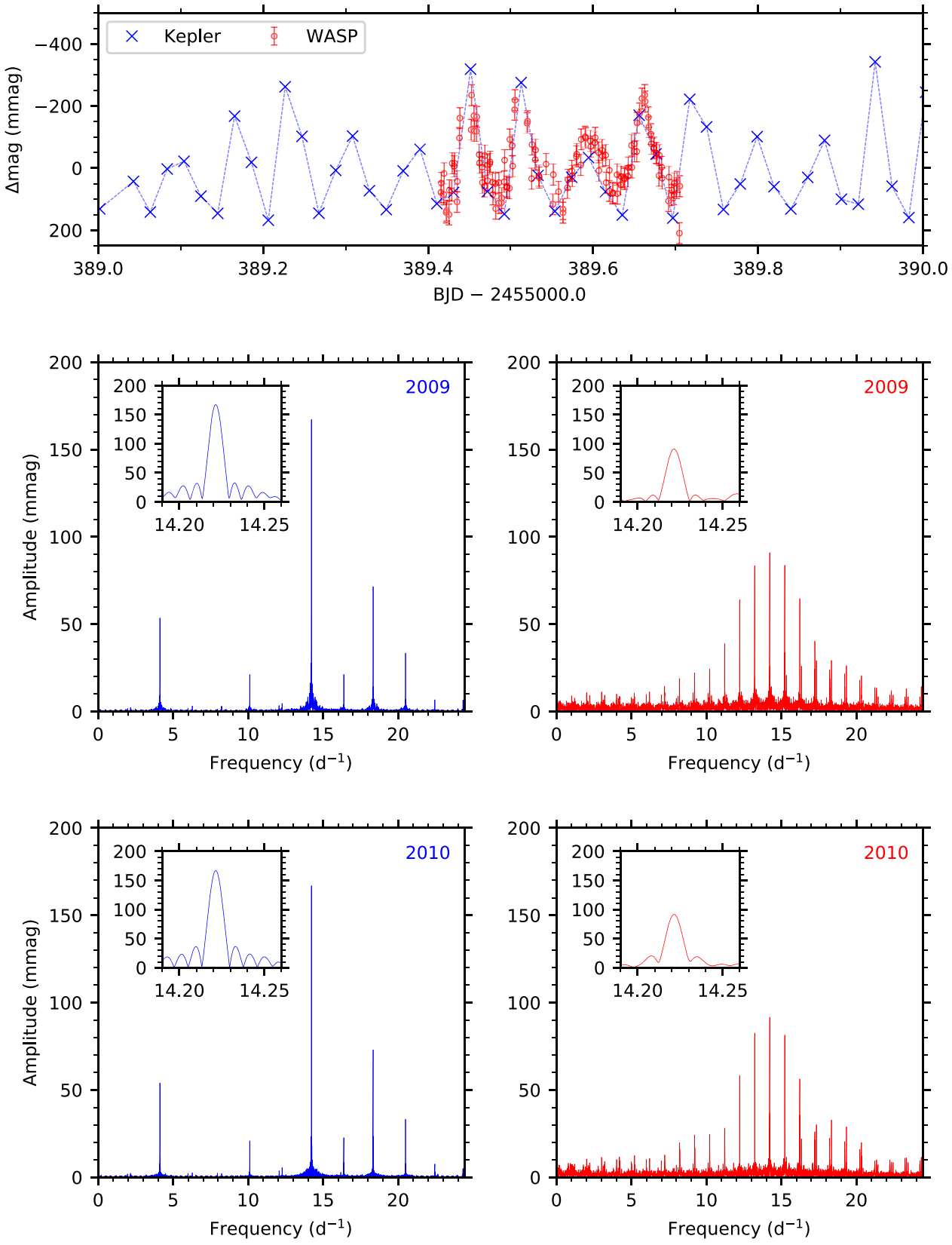

Figure 2. The top panel is a 1-d segment of the *Kepler* and WASP light curves of KIC 5950759 shown as blue crosses and red circles, respectively. The lower panels show amplitude spectra of KIC 5950759 labelled by their respective observing season, with the left-hand panels denoting *Kepler* data in blue and the right-hand panels denoting WASP data in red. In each panel, a sub-plot of the dominant pulsation mode frequency, ν_1, is shown. The lower amplitudes of the pulsation modes in the WASP data are primarily caused by flux dilution in the relatively larger WASP pixels (see text for details).

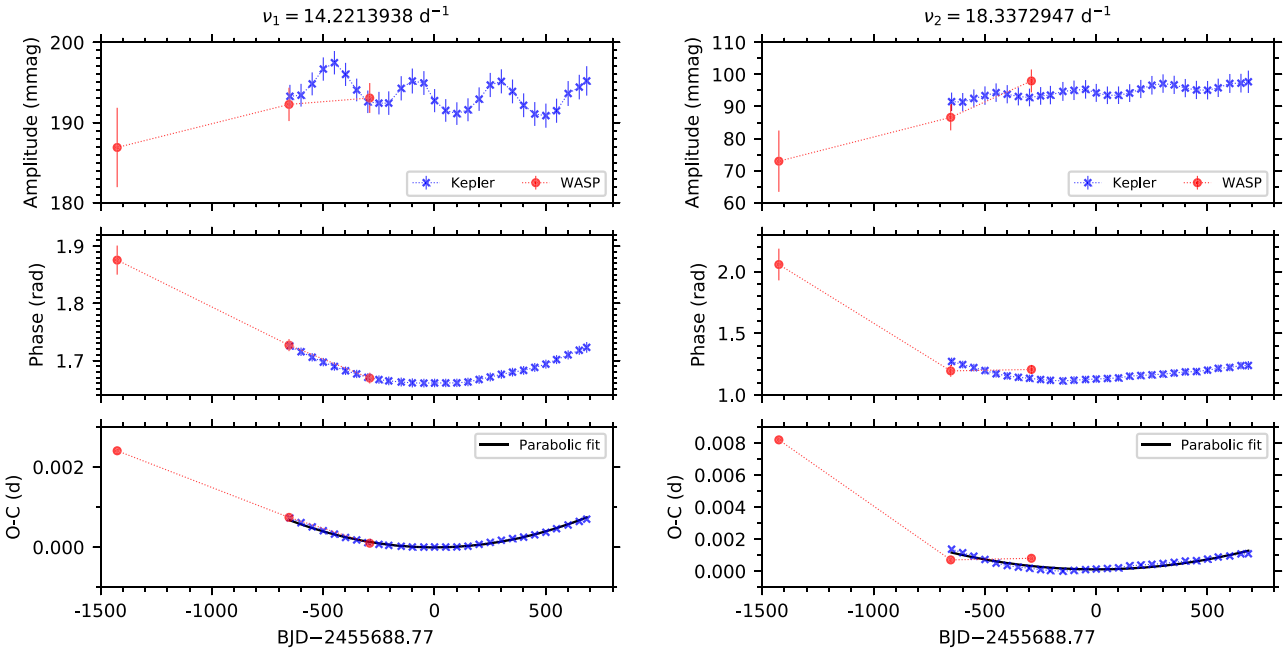

Figure 3. Inclusion of WASP data with *Kepler* data to study the long-term amplitude and phase modulation of the fundamental, ν_1 (left), and first overtone, ν_2 (right), radial modes in KIC 5950759. Top panels: amplitude modulation in KIC 5950759 using the available LC *Kepler* data (in bins of 150 d and 100-d overlap) as blue crosses and the three WASP seasons as red circles, which have been corrected for their respective integration times, passbands, and dilution (see text for details). Middle panels: phase modulation tracked at fixed frequency. Bottom panels: O − C diagram in which the parabolic fit reveals the linear rate of change in period for each pulsation mode. In all panels, the zero-point of the time scale has been taken as the centre of the LC *Kepler* data set (i.e. BJD 2455688.770). Note that the bottom two rows are equivalent.

is understandable given the difference in passband between the two instruments and because pulsation phases depend on wavelength.[5]

After correcting the 2007, 2009, and 2010 WASP phases for the passband phase offset value, we include them alongside the LC *Kepler* data of KIC 5950759 in the middle panels of Fig. 3. A clear parabolic change in pulsation phase is evident for both the fundamental (ν_1; middle-left panel of Fig. 3) and first overtone (ν_2; middle-right panel of Fig. 3), which indicate a linearly increasing pulsation period. Under the reasonable assumption of negligible mass-loss across a period of approximately 6 yr, this implies an increasing stellar radius in KIC 5950759. The observed phase modulation for each radial mode, ν_1 and ν_2, is converted using $\mathrm{O-C} = \frac{\phi}{2\pi\nu}$, with the resultant O − C diagrams shown in the bottom-left and bottom-right panels of Fig. 3, respectively. To avoid adding unnecessary additional uncertainty, we fit only the *Kepler* data with equation (4) with $(\frac{1}{P}\ \frac{\mathrm{d}P}{\mathrm{d}t})$ as a free parameter. The fitted fractional rate of change in period values have units of d^{-1} since t and O − C are in units of d, we converted them into the conventional unit of yr^{-1}. This yielded best-fitting values of $(1.17 \pm 0.02) \times 10^{-6}$ yr^{-1} and $(1.82 \pm 0.12) \times 10^{-6}$ yr^{-1} for the fractional period changes of the fundamental and first overtone radial modes, respectively.

Contrary to stellar evolution theory, approximately an equal fraction of Population I δ Sct stars are observed to have increasing periods compared to those with decreasing periods in their radial modes (Breger 1990; Guzik & Cox 1991). The typical linear period changes observed in δ Sct stars can be as large as $\dot{P}/P \simeq 10^{-7}$ yr^{-1}, which is at least an order of magnitude larger than those predicted by stellar evolution theory for main sequence δ Sct stars (Breger & Pamyatnykh 1998). Similarly, large period changes have also been observed in HADS stars (e.g. Walraven et al. 1992) and SX Phe stars (e.g. Murphy et al. 2013b). In KIC 5950759, we measure even larger period changes of order 10^{-6} yr^{-1}, which could be used to infer that this HADS star is in a relatively short-lived stage of stellar evolution, such as near or beyond the TAMS, if such variability is caused by evolution. The increasing period of the radial modes also implies that the radius of KIC 5950759 is increasing, which suggests a post-main-sequence stage of evolution as opposed to the overall contraction phase. An order of magnitude estimate of the change in radius using the period–density relation for classical pulsators (see e.g. Stellingwerf 1979) and assuming a constant mass of $M = 1.6$ M$_\odot$ yields $\dot{R} \simeq 1$ km yr^{-1}, but the uncertainties on this are substantial. Such a value is three orders of magnitude larger than expected from stellar evolution models. Hence, it is unlikely that the observed period (and implied radius) changes are caused by evolution.

We note that the amplitude and phase modulation observed in KIC 5950759 are seemingly unique, because phase modulation in such stars appears as jumps rather than smooth variation over time (see e.g. Breger & Pamyatnykh 1998; Boonyarak et al. 2011). On the other hand, few HADS stars have been studied using such high quality photometric time series as those provided by the *Kepler* mission. Since the observed phase modulation is much larger than predicted by evolution models, this indicates that the short-term evolution of some stars can be quite *'noisy'*, such that period changes measured over time spans of years and decades may be caused by physical processes that are not resolved by the large time steps taken in evolutionary calculations.

[5]Pulsation mode phase differences is a method of mode identification for multicolour time series photometric observations – see Watson (1988) and Heynderickx, Waelkens & Smeyers (1994) for early applications of this technique.

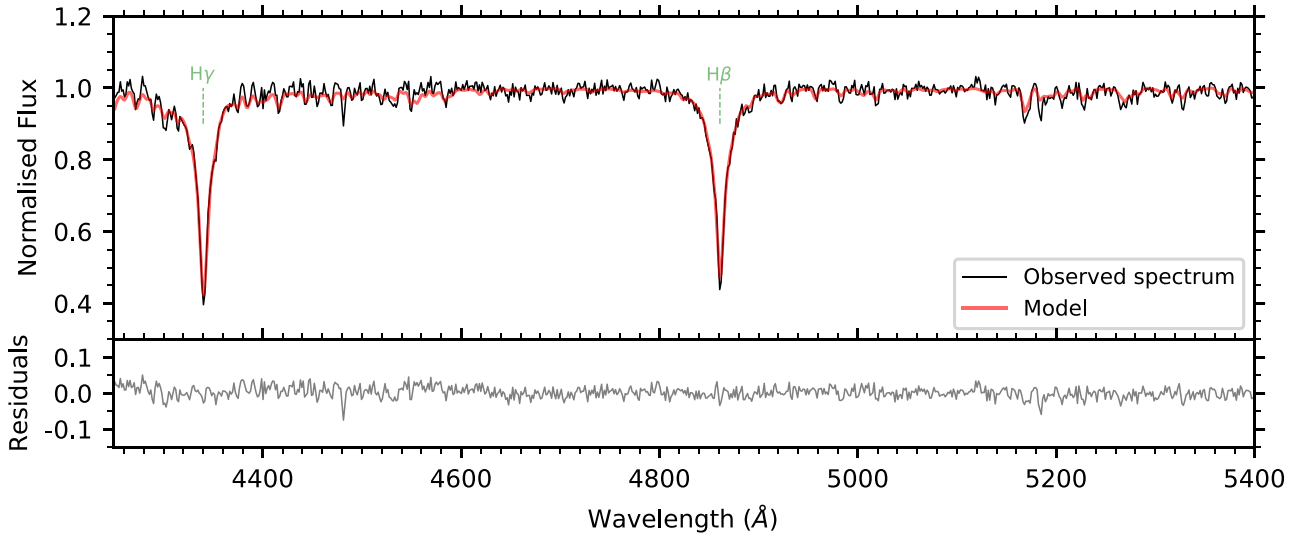

Figure 4. Top panel: observed spectrum of KIC 5950759 (black) and the best-fitting model (without continuum correction) obtained using the GSSP software (Tkachenko 2015) in red. Bottom panel: residuals of model and observations.

3 SPECTROSCOPY

KIC 5950759 is a relatively faint star within the nominal *Kepler* field of view with $V = 13.516$ mag (Pigulski et al. 2009). To determine atmospheric parameters, and in particular an accurate effective temperature, $T_{\rm eff}$, we obtained a spectrum on 2016 September 28 using the Intermediate Dispersion Spectrograph (IDS) mounted on the 2.5-m Isaac Newton Telescope (INT) located at the Roque de los Muchachos Observatory on the island of La Palma, Spain. The spectrum was obtained using the R400V grating with a resolving power of $R \simeq 1500$ at 4500 Å. We reduced the data (including bias subtraction, flat-fielding, and wavelength calibration) using STARLINK[6] software (Currie et al. 2014). We normalized the spectrum by fitting a spline through manually selected continuum points. A section of the normalized reduced IDS spectrum of KIC 5950759 is shown in Fig. 4. Spectral classification indicates that KIC 5950759 is a slow rotator from its narrow spectral lines, and is also a metal-poor A-type star given the lack of strong metal lines (Gray 2005; Gray & Corbally 2009).

To analyse the spectrum of KIC 5950759 using a quantitative method and extract atmospheric parameters, we used the Grid Search in Stellar Parameters (GSSP) software (Tkachenko 2015). The GSSP code computes a grid of synthetic spectra across a range of values in effective temperature ($T_{\rm eff}$), surface gravity ($\log g$), metallicity ([M/H]), and projected surface rotational velocity ($v \sin i$). The grid of synthetic spectra is computed using the SYNTHV LTE radiative transfer code (Tsymbal 1996) and atmospheric models computed from the LLMODELS code (Shulyak et al. 2004). In our analysis, we fix the microturbutent and macroturbutent velocities to 2.0 and 0.0 km s^{-1}, respectively, which are reasonable for stars of spectral type A (Gray 2005; Tkachenko et al. 2013; Niemczura et al. 2015). As mentioned previously, the low resolution of the observed spectrum makes it difficult to constrain the surface gravity and rotation rate of KIC 5950759. Furthermore, for stars below approximately 8000 K, the wings of Balmer lines are not sensitive to the surface gravity, which means that metal lines are typically used instead (Gray 2005; Smalley 2005). Given the resolving power of the IDS/INT instrument and the resultant resolution of the observed spectrum, rotational and instrumental broadening are indistinguishable for $v \sin i$ values below some 50 km s^{-1}.

We shifted the observed spectrum to rest wavelengths and used the GSSP code to quantitatively compare it to each spectrum within the grid of synthetic spectra by means of minimizing the corresponding χ^2 function. After some initial tests, we confirmed that KIC 5950759 is a slow rotator, with $v \sin i \lesssim 50$ km s^{-1}, such that the inferred rotational broadening was smaller than the instrumental broadening. Therefore, we set the velocity broadening component to 0 km s^{-1} when using GSSP in our subsequent analysis. As a first step, we use the 4250–5400 Å wavelength range to constrain the effective temperature to $T_{\rm eff} = 7340 \pm 230$ K, which is primarily driven by the shape of the H γ and H β Balmer lines in this range. Given the low resolution of the spectrum and lack of strong metal lines, we are unable to constrain the surface gravity to better than $\log g = 2.9 \pm 1.3$ dex and metallicity to [M/H] $= -1.18 \pm 0.30$ dex. As a second step, we performed a second fitting scheme including a global continuum correction factor, which is assumed to be wavelength-independent and is computed in GSSP from the least-squares fit of the synthetic to the observed spectrum of the star. For the same wavelength regime of 4250–5400 Å, we constrained the effective temperature to $T_{\rm eff} = 7470 \pm 255$ K, the surface gravity to $\log g = 3.6 \pm 1.2$ dex and the metallicity to [M/H] $= -0.65 \pm 0.45$ dex. These parameters are consistent with those from our previous analysis, and are provided in Table 1.

As an additional confirmation of the sub-solar metallicity of KIC 5950759, we estimated the metallicity using the methodology of Smalley (1993). An estimate of the line blocking in the 4600–4700 Å region using a model with $T_{\rm eff} = 7500$ K and $\log g = 3.5$ yielded a metallicity of [M/H] $= -1.1 \pm 0.4$, which is consistent with the sub-solar metallicity values obtained from GSSP. The high frequency of the fundamental radial mode in KIC 5950759, and the relatively large observed frequency ratio of 0.77554 also support that KIC 5950759 is a metal-poor star (see e.g. Petersen & Christensen-Dalsgaard 1996; Poretti 2003; Murphy et al. 2013b; Daszyńska-Daszkiewicz et al. 2020).

[6] http://starlink.eao.hawaii.edu/starlink/

4 ESTIMATING THE LUMINOSITY FROM GAIA

In their study of the P–L relation for δ Sct stars observed by *Kepler* with available *Gaia* parallaxes, Ziaali et al. (2019) include KIC 5950759 as an example of a star known to pulsate in the fundamental radial mode (see their fig. 3). Interestingly, KIC 5950759 does not fall on the derived P–L relationship. Owing to the pulsation period being known to an extremely high precision, the discrepancy may be caused by an incorrect luminosity from an incorrect estimate of the interstellar reddening and/or distance. Murphy et al. (2019) calculated luminosities for a large sample of more than 2000 δ Sct stars observed by the *Kepler* mission with available *Gaia* DR2 parallaxes (Gaia Collaboration 2016, 2018), distances from Bailer-Jones et al. (2018) and dust maps from Green et al. (2018). From their ensemble analysis, Murphy et al. (2019) calculated a luminosity of $\log(L/\mathrm{L}_\odot) = 1.017 \pm 0.038$ for KIC 5950759 assuming an effective temperature $T_{\rm eff} = 8070 \pm 280$ K.

The bolometric corrections of Murphy et al. (2019) were calculated based on parameters available from the Mathur et al. (2017) stellar properties catalogue, which are somewhat consistent with those found in this work except for the metallicity, which we find to be sub-solar with $-1.18 < [\mathrm{M/H}] < -0.65$ dex (cf. Table 1). This can have a large effect on the bolometric correction, so we have re-calculated the luminosity using the updated astrometry from *Gaia* EDR3 (Gaia Collaboration 2021), the effective temperatures, surface gravities and metallicities from our spectroscopic analysis, which yields $\log(L/\mathrm{L}_\odot) = 1.064 \pm 0.045$. The fractional distance uncertainty for KIC 5950759 is ∼4 per cent, whereas the fractional uncertainty on the 0.22 mag extinction value is 16 per cent. Thus neither of these parameters is a likely source of the ≃0.2 mag difference between the calculated absolute magnitude of KIC 5950759 and the inferred P–L relation in Ziaali et al. (2019).

A potential cause of a star appearing too bright in the P–L diagram is binarity. The *Gaia* renormalized unit weight error (RUWE) has been interpreted as an indication of binarity, with RUWE >2 used to suggest binarity (Evans 2018; Rizzuto et al. 2018). In *Gaia* EDR3, the RUWE parameter for KIC 5950759 is 1.047, so it is probably not a binary. Furthermore, after comparing the *Gaia* DR2 astrometric excess noise of 0.11 mas for KIC 5950759 to the average DR2 excess noise of 0.14 mas for the large sample of *Kepler* A and F stars from Murphy et al. (2019), we conclude that KIC 5950759 is unlikely to be a binary.

More importantly, McNamara (2011) found that corrections to the P–L relation were required for low-metallicity radial-mode pulsators. For stars of $[\mathrm{Fe/H}] \simeq -1.0$, a correction of 0.2 mag is required, such that a star is overluminous by this amount compared to the luminosity predicted solely based on its dominant pulsation period (McNamara 2011). This correction would account for the location of KIC 5950759 being above the P–L relation found by Ziaali et al. (2019) for *Kepler* δ Sct stars. On the other hand, we cannot exclude an incorrect extinction for KIC 5950759 given its faint apparent brightness and larger inferred *Gaia* distance compared to typical A and F stars in the *Kepler* field.

Finally, we note that the large pulsation amplitude of KIC 5950759 causes substantial temperature, radius, and radial velocity variations during the pulsation cycle. Using equation (5) of Kjeldsen & Bedding (1995), we estimate radial velocity variability of $\sim$100 km s^{-1} for measured brightness variations of $\pm$0.4 mag, given that in *Kepler* SC data the peak-to-peak light amplitude variations exceed 0.7 mag. We did not include the radius and temperature variations in the 10 000-iteration Monte Carlo simulation for our improved calculation of the luminosity of KIC 5950759 in this work. Yet, we did include a 1σ apparent magnitude change of 0.14 mag calculated from the standard deviation of the *Kepler* brightness measurements.

5 ASTEROSEISMIC MODELLING

To ascertain the mass and evolutionary stage of KIC 5950759, we performed forward seismic modelling based on its observed pulsation mode frequencies, spectroscopic parameters and *Gaia* luminosity. Since *Kepler* data are of exceptionally high quality, the two dominant pulsation mode frequencies and their frequency ratio are known to a very high precision. The high amplitudes of the pulsation modes and their frequency ratio indicate that they are likely the fundamental and first overtone radial modes, so a sensible method to model KIC 5950759 is by using Petersen diagrams. The frequency and frequency ratio of radial modes depend primarily on the mass, age, evolutionary stage, and metallicity. Thus, Petersen diagrams offer a useful diagnostic in constraining these parameters of radial pulsators (see e.g. Petersen 1973; Petersen & Christensen-Dalsgaard 1996; Daszyńska-Daszkiewicz et al. 2020).

We calculated evolution models with the WARSAW-NEWJERSEY code (see Pamyatnykh et al. 1998; Pamyatnykh 1999) using the OPAL opacity tables (Iglesias & Rogers 1996) and a solar chemical mixture (Asplund et al. 2009) for various metallicity values. Rotation, or more specifically the mean effect of the centrifugal force, is included within the WARSAW-NEWJERSEY code, and solid-body rotation and constant global angular momentum during evolution are assumed. Convection in the stellar envelope is based on standard mixing length theory, and the convective flux is assumed to be constant throughout a pulsation cycle. This is more commonly known as the convective flux freezing approximation, which is robust if convection is not efficient, such as in the envelopes of early type stars. Linear non-adiabatic pulsation models were calculated using the code of Dziembowski (1977).

As described in Section 3, there are large uncertainties associated with determining the metallicity of a slowly rotating, high-amplitude pulsating star with a low-resolution spectrum. Therefore, we chose to survey a range of models with different metallicities between $0.004 \leq Z \leq 0.013$ dex in steps of 0.001 dex, which is larger than the inferred 1σ metallicity uncertainty from spectroscopy, and determine the best-fitting mass and age. For each value of metallicity, we found the model that fits the dominant frequency (ν_1) identified as the fundamental radial mode, and closely matches the frequency identified as the first overtone radial mode (ν_2). Our results are shown in the mass-metallicity plane in Fig. 5. All the models in Fig. 5 match the observed frequencies ν_1 and ν_2, which demonstrates the strong mass-metallicity degeneracy. In general, fitting the two pulsation modes alone is unable to break the degeneracy between mass and age.[7] Hence one needs additional information, such as fitting a third mode or including spectroscopic constraints, to constrain the age of a star. Specifically, effective temperature and metallicity derived from spectroscopy and the luminosity estimated from *Gaia* are used to delimit the possible parameter space in the HR diagram.

As can be seen in Fig. 5, there are two branches of possible solutions for KIC 5950759: main-sequence models for which $Z \geq 0.008$ and post-main-sequence models for which $0.004 \leq Z < 0.007$.

[7] Analogous to isochrones (lines of constant age), one can fit isopycnals or isopycnics (i.e. lines or surfaces of constant density) using frequency ratios of radial modes (see Hermans 2019) to serve as a proxy for stellar age in the HR diagram as opposed to using uncertain spectroscopic log g values.

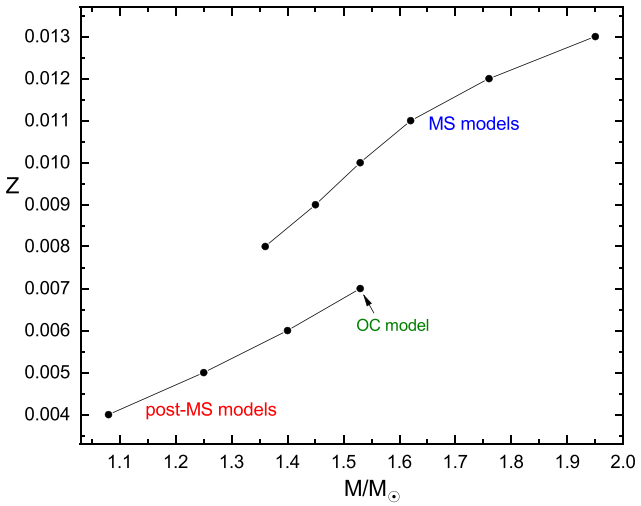

Figure 5. Models calculated across a range in metallicity which match the observed frequency ratio observed in KIC 5950759. The strong constraint of the observed frequency ratio creates two branches in terms of possible evolutionary phases (where MS = main sequence, OC = overall contraction phase, post-MS = post-main sequence).

For each model at a given metallicity shown in Fig. 5, we provide the best-fitting mass, age, effective temperature, luminosity, theoretical frequency of the first overtone radial mode, and the frequency ratio of the fundamental and first overtone radial modes in Table 3. For each best-fitting model, we also calculate the normalized instability parameters $\eta(p_1)$ and $\eta(p_2)$ (as defined by Stellingwerf 1978; see also Daszyńska-Daszkiewicz et al. 2020), for which positive values indicate that a pulsation mode is excited (i.e. unstable) and negative values indicate it is not (i.e. stable).

However, not all models shown in Fig. 5 lie within 3σ of the spectroscopic constraints on the effective temperature and *Gaia* luminosity for KIC 5950759. To demonstrate the importance of these additional constraints in forward seismic modelling, we show Petersen diagrams for different parameter combinations in Fig. 6. In the top panel, Petersen diagrams for extremely metal-poor stars are shown as coloured lines; none of which match the observed frequency ratio of KIC 5950759. On the contrary, the observed frequency ratio excludes the possibility of KIC 5950759 having $Z < 0.003$, with the lowest value in our grid that matches the frequency ratio being $Z = 0.004$. At the other end of the metallicity scale are main-sequence models with higher masses and younger ages that match the observed frequency ratio of KIC 5950759. We show an example of a near-solar metallicity (i.e. $Z = 0.012$) Petersen diagram in the bottom panel of Fig. 6. Therefore, the metallicity of KIC 5950759 must lie within the range of $0.004 \leq Z \leq 0.013$, if one only considers the fit using only the fundamental and first overtone radial mode frequencies. In Fig. 7, we show the position of KIC 5950759 with its 3σ error box and seismic models with the corresponding evolutionary tracks for several metallicities. In the left-hand panel, we marked seismic models in the post-main-sequence phase of evolution and in the right-hand panel seismic models in main-sequence phase of evolution. The location of KIC 5950759 in the HR diagram combined with the best-fitting frequency ratio of its fundamental and first overtone radial modes indicates a relatively low-mass star ($M \lesssim 1.6$ M$_\odot$) with sub-solar metallicity near the overall contraction phase and the TAMS.

We also explored including convective core overshooting as a parameter in our models. The WARSAW-NEWJERSEY code uses a two parameter prescription introduced by Dziembowski & Pamyatnykh (2008), which allows for a non-zero gradient of the hydrogen abundance inside the partly mixed region above the convective core. An example of the effect of overshooting with the efficiency parameter $\alpha_{ov} = 0.25$ for $Z = 0.006$ is shown in the middle panel of Fig. 6. Increasing the amount of near-core mixing provides the convective core with additional hydrogen available for nuclear burning during the main sequence. This extends the main-sequence lifetime of the star and moves the location of the TAMS and blue hook to larger radii and hence higher luminosities in the HR diagram. Consequently, it also moves the TAMS to smaller frequency ratios in the Petersen diagram. Therefore, for $Z = 0.006$, as shown in the middle panel of Fig. 6 and listed in Table 3, the best-fitting model with $Z = 0.006$ and $\alpha_{ov} = 0.00$ is a post-main-sequence star, and with $Z = 0.006$ and $\alpha_{ov} = 0.25$ it is a main-sequence star.

A major advantage of using non-adiabatic pulsation models is that we are also able to determine if modes are excited. As can be seen in Table 3, the normalized instability parameters, $\eta(p_1)$ and $\eta(p_2)$, are negative for $Z \geq 0.012$, which means we can exclude relatively high mass (i.e. $M \geq 1.7$ M$_\odot$) main-sequence models as we do not expect the fundamental and first overtone radial modes to be

Table 3. The parameters of the models that reproduce exactly the observed dominant frequency ν_1 as the radial fundamental mode ($\ell = 0,\ p_1$) and closely match the observed frequency ν_2 as the radial first overtone ($\ell = 0,\ p_2$). All models have an initial hydrogen abundance of $X_0 = 0.70$, mixing length parameter $\alpha_{MLT} = 0.1$ and an initial rotational velocity $v_{rot} = 10$ km s^{-1}. Columns are metallicity (Z), the convective core overshooting (α_{ov}), mass (M), phase of evolution (where OC denotes the overall contraction phase), age, effective temperature ($\log T_{eff}$), luminosity ($\log L/L_\odot$), the theoretical frequency of the radial first overtone $\nu(p_2)$, the frequency ratio of the first two radial modes and their normalized instability parameters $\eta(p_1)$ and $\eta(p_2)$, and the theoretically predicted fractional period change of the fundamental radial mode.

Z	α_{ov}	M (M$_\odot$)	phase	age (Gyr)	$\log T_{eff}$	$\log L/L_\odot$	$\nu(p_2)$ (d^{-1})	$\nu(p_1)/\nu(p_2)$	$\eta(p_1)$	$\eta(p_2)$	$\dot{P}/P$ (yr^{-1})
0.004	0.0	1.08	post-MS	3.66	3.8285	0.743	18.33686	0.77556	+0.079	+0.036	$+8.5 \times 10^{-10}$
0.005	0.0	1.25	post-MS	2.25	3.8652	0.932	18.33704	0.77556	+0.068	+0.066	$+1.2 \times 10^{-9}$
0.006	0.0	1.40	post-MS	1.62	3.8919	1.071	18.33817	0.77551	−0.029	+0.015	$+1.0 \times 10^{-9}$
0.006	0.25	1.21	MS	2.60	3.8195	0.737	18.33857	0.77549	+0.070	+0.024	$+6.1 \times 10^{-10}$
0.007	0.0	1.53	OC	1.31	3.9099	1.167	18.33867	0.77549	−0.143	−0.071	-2.3×10^{-8}
0.008	0.0	1.36	MS	1.73	3.8359	0.835	18.33685	0.77556	+0.082	+0.045	$+7.7 \times 10^{-10}$
0.009	0.0	1.45	MS	1.42	3.8510	0.914	18.33668	0.77557	+0.079	+0.058	$+8.2 \times 10^{-10}$
0.010	0.0	1.53	MS	1.21	3.8637	0.979	18.33759	0.77553	+0.059	+0.058	$+8.8 \times 10^{-10}$
0.011	0.0	1.62	MS	1.02	3.8775	1.051	18.33797	0.77552	+0.016	+0.038	$+9.4 \times 10^{-10}$
0.012	0.0	1.76	MS	0.78	3.9014	1.170	18.33771	0.77555	−0.104	−0.048	$+1.1 \times 10^{-9}$
0.013	0.0	1.95	MS	0.56	3.9324	1.323	18.33985	0.77544	−0.326	−0.256	$+1.3 \times 10^{-9}$

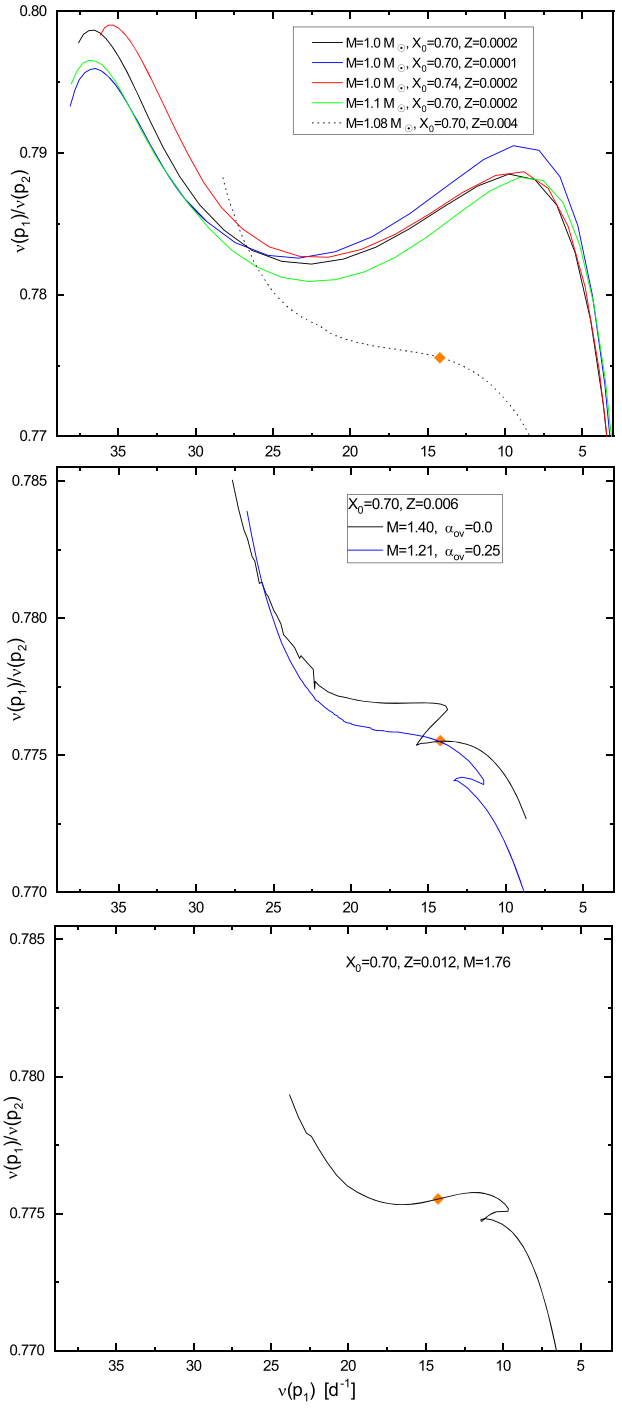

Figure 6. Petersen diagrams spanning from the ZAMS to the immediate post-main-sequence phase of evolution for various metallicity values in our grid. In each panel, the location of the best model is indicated by the orange diamond. The observed frequency ratio of ν_1/ν_2 for KIC 5950759 clearly excludes low metallicities (i.e. $Z < 0.003$).

excited. Furthermore, the best-fitting model for $Z = 0.007$ also has negative $\eta(p_1)$ and $\eta(p_2)$ values, which means that we can exclude the overall contraction phase. Combining the requirement for positive normalized instability parameters with the 3σ confidence intervals for $T_{\rm eff}$ and log L for KIC 5950759, the best-fitting models are those with metallicity values approximately in the two ranges of $Z \in (0.005, 0.006) \cup (0.010, 0.011)$. However, our best-fitting models consistently place KIC 5950759 near to the TAMS.[8] Given this result and the limitations and uncertainties associated with the determination of $T_{\rm eff}$, $v \sin i$, and Z for KIC 5950759, it is highly desirable that high-resolution spectra of KIC 5950759 be obtained. Preferably spectra sampling the pulsation cycle of ν_1 should be obtained. This will allow a more accurate determination of the metallicity and effective temperature given that the large amplitude pulsations of KIC 5950759 are likely causing significant line broadening which cannot be taken into account in the analysis of only a single spectrum.

Motivated by the large observed values for the fractional period change in the fundamental and first overtone radial modes, we also checked the theoretically predicted values within our models for agreement. For completeness, we extracted the fractional period change of the fundamental radial mode of the best-fitting model at each metallicity value in our grid. These values are provided in the last column of Table 3. The values are similar for the first overtone radial mode, and also comparable to those calculated by Breger & Pamyatnykh (1998). Yet, all predicted values are considerably smaller than the fractional period change observed in KIC 5950759 by at least two orders of magnitude. It is well established that δ Sct stars (both Population I and II) have observed period changes much larger than predicted by evolutionary models (Rodríguez et al. 1995; Breger & Pamyatnykh 1998; Rodríguez & Breger 2001; Bowman et al. 2016). Therefore, we conclude that the (common) observed period changes in δ Sct pulsators are not the result of stellar evolution, but are likely connected to the inherent non-linear excitation mechanism of high-amplitude pulsation modes, and the interactions of modes causing modulated amplitudes and frequencies over time-scales of years and decades (e.g. resonant mode coupling; Dziembowski & Krolikowska 1985; Moskalik 1985; Breger & Montgomery 2014; Bowman et al. 2016). Therefore, our results demonstrate the need for future studies to move beyond linear asteroseismology, and include additional constraints based on pulsation amplitudes and non-linear effects at work in δ Sct stars.

6 CONCLUSIONS

In this work, we have performed photometric, spectroscopic, and modelling analyses of the high-amplitude δ Sct star KIC 5950759. Originally identified as having unique properties owing to its long term and large fractional period change in its fundamental radial and first overtone radial modes by Bowman (2016), our detailed frequency analysis of the *Kepler* mission photometry of KIC 5950759 reveals additional non-radial pulsation modes. We extend the 4-yr time span of the *Kepler* mission using WASP data, and demonstrate that KIC 5950759 exhibits long-term amplitude and phase modulation in its two dominant radial modes. The measured fractional linearly increasing periods of the fundamental and first overtone radial mode are of the order of 10^{-6} yr^{-1}, which are at least two orders of magnitude larger than predicted for evolutionary changes in main sequence and post-main sequence stars. Given such a large discrepancy is not supported by stellar evolution models, we conclude that non-linear mode interaction is an explanation for the time-dependent phenomena observed in KIC 5950759, as predicted by Dziembowski & Krolikowska (1985) and Moskalik (1985).

[8]Note that the TAMS as defined by Iben (1967) is before the overall contraction phase and blue hook in the HR diagram, such that $X_c \simeq 0.05$. Whereas other studies, such as Dotter (2016), define the TAMS as when the core hydrogen content (numerically) reaches zero.

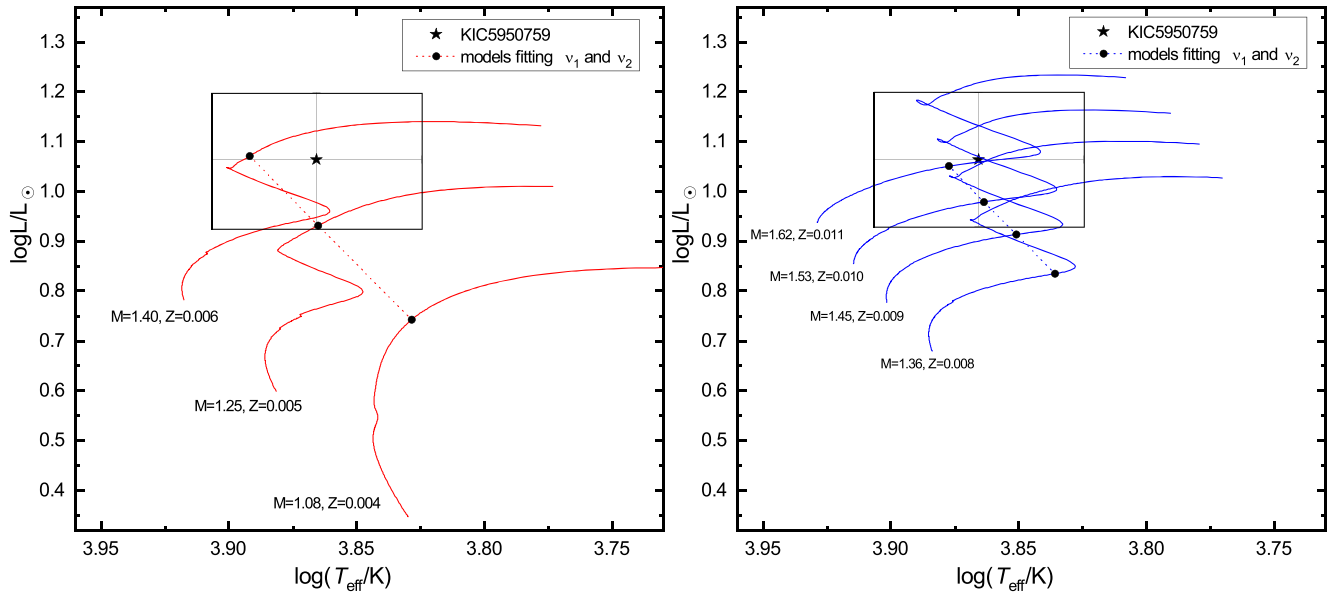

Figure 7. HR diagram with the $3\sigma\, T_{\rm eff} - \log\, L$ error box of KIC 5950759 and evolutionary tracks computed for various masses and metallicities at the adopted values of an initial hydrogen abundance $X_0 = 0.7$, the mixing length parameter $\alpha_{\rm MLT} = 0.1$ and no convective core overshooting. Seismic models that best reproduce the two dominant frequencies as the fundamental and first overtone radial modes are marked with dots. In the left-hand panel, the best-fitting seismic models are in the post-main-sequence phase of evolution and in the right-hand panel they are in main-sequence phase of evolution.

We obtained and analysed low-resolution spectroscopy of KIC 5950759 using the GSSP software package (Tkachenko 2015). The determined effective temperature places KIC 5950759 within the predicted and observed instability region for δ Sct stars (see Murphy et al. 2019), albeit somewhat closer to the red edge but none the less within the typical parameter space of high-amplitude δ Sct stars (Petersen & Christensen-Dalsgaard 1996; McNamara 2000a). On the other hand, our spectroscopic analysis was unable to accurately constrain the rotational velocity of KIC 5950759 owing to the total broadening being smaller than the instrumental broadening. Also, the low resolution of the spectrum increased the uncertainties associated with determining the surface gravity and metallicity of KIC 5950759, but the best-fitting values provided by GSSP are given in Table 1. We compared previous determinations of the luminosity of KIC 5950759 by Murphy et al. (2019) to new calculations based on *Gaia* EDR3 parameters (Gaia Collaboration 2021) and conclude that KIC 5950759 is a single star as opposed to a binary.

Using the observed pulsation mode frequencies from the *Kepler* mission data, the spectroscopic constraints on $T_{\rm eff}$ and metallicity, the *Gaia* luminosity, and the normalized instability parameters for the fundamental and first overtone, we determined the most likely masses and ages of KIC 5950759 using forward seismic modelling based on Petersen diagrams. Our results are summarized in Table 3. We find that the best-fitting seismic models considering all the available constraints exist within two branches of the sub-solar metallicity regime [i.e. $Z \in (0.005, 0.006) \cup (0.010, 0.011)$]. Our spectroscopic metallicity favours the lower-metallicity range in our models (i.e. $Z \in (0.005, 0.006)$, which further strengthens the conclusion that KIC 5950759 is near the TAMS. Multi-epoch high-resolution spectroscopy that effectively samples the dominant pulsation cycle of KIC 5950759 is needed to accurately determine its atmospheric parameters. Large amplitude pulsations induce significant changes in the effective temperature and radius of a star, and such behaviour is not captured within our analysis of a single low resolution spectrum.

Most interestingly, the relatively large increasing period changes in the fundamental and first overtone radial modes combined with our modelling results indicates that such an observed period change is too large to be caused directly by stellar evolution. This is in agreement with observations of δ Sct stars from the ground (see e.g. Breger & Pamyatnykh 1998). Our modelling results indicate that KIC 5950759 is close to, if not just past, the TAMS. Despite this being the parameter space where period changes caused by evolution are predicted to be maximal, the observed amplitude and phase modulation of KIC 5950759 is too large to be directly caused by evolution. Given that the high-amplitude pulsations of HADS stars are sufficient to drive a periodic change in the stellar radius of the order of a factor two every $\simeq$2 h, we posit that the observed amplitude and phase modulation is the manifestation of the star's structure responding to a highly non-linear driving mechanism. Post-main-sequence δ Sct or post-main-sequence HADS stars are not uncommon, but since HADS stars themselves make up only a small minority of all A and F stars, this only lends further evidence that KIC 5950759 is a unique object within all the known δ Sct stars observed by the *Kepler* mission.

In the future, we expect ongoing space photometry missions, such as *TESS* (Ricker et al. 2015), to find additional interesting HADS stars in, or close to, relatively short lived stages of stellar evolution. Currently, it is difficult to study the evolutionary changes in δ Sct stars from their pulsations in real time as they occur on such long time-scales compared to observations. Moreover, non-linear mode interactions causing significant amplitude and phase modulation seemingly dominate their temporal behaviour (Breger 2000c; Bowman & Kurtz 2014; Breger & Montgomery 2014; Bowman et al. 2016). However, for relatively short-lived phases of evolution, such as the overall contraction phase and the immediate post-main sequence, with a large enough sample of δ Sct stars observed by *TESS*, we should expect to increase this sample size to a non-negligible number of candidates. Ultimately, a large enough sample of pulsating stars with similar temporal properties to KIC 5950759 will allow us to probe

non-linear pulsations and their effect on stellar structure in real time across a range of stellar masses and metallicities, and determine why such large period changes are present in so many δ Sct stars, but not in all.

ACKNOWLEDGEMENTS

DMB gratefully acknowledges a senior postdoctoral fellowship from the Research Foundation Flanders (FWO) with grant agreement no. 1286521N. JDD acknowledges support from the Polish National Science Center (NCN), grant no. 2018/29/B/ST9/02803. DLH acknowledges the Science and Technology Facilities Council (STFC) via grant ST/M000877/1. SJM is a DECRA fellow supported by the Australian Research Council, grant number DE180101104. This work was supported by the Australian Research Council, an Australian Government Research Training Program (RTP) scholarship, and the Danish National Research Foundation (Grant DNRF106) through its funding for the Stellar Astrophysics Centre (SAC). The research leading to these results has received funding from the European Research Council (ERC) under the European Union's Horizon 2020 research and innovation programme (grant agreement no. 670519: MAMSIE), from the KU Leuven Research Council (grant C16/18/005: PARADISE), from the Research Foundation Flanders (FWO) under grant agreements G0H5416N (ERC Runner Up Project), as well as from the BELgian federal Science Policy Office (BELSPO) through PRODEX grant PLATO.

The *Kepler* data presented in this paper were obtained from the Mikulski Archive for Space Telescopes (MAST) at the Space Telescope Science Institute (STScI), which is operated by the Association of Universities for Research in Astronomy, Inc., under NASA contract NAS5-26555. Support to MAST for these data is provided by the NASA Office of Space Science via grant NAG5-7584 and by other grants and contracts. Funding for the Kepler/K2 mission was provided by NASA's Science Mission Directorate. The *Gaia* data in this paper come from the European Space Agency mission Gaia, processed by the *Gaia* Data Processing and Analysis Consortium (DPAC). Funding for the DPAC has been provided by national institutions, in particular the institutions participating in the *Gaia* Multilateral Agreement. The WASP project is funded and operated by Queen's University Belfast, the Universities of Keele, St. Andrews and Leicester, the Open University, the Isaac Newton Group, the Instituto de Astrofísica de Canarias, the South African Astronomical Observatory, and by STFC.

This research made use of the STARLINK software (Currie et al. 2014), which is currently supported by the East Asian Observatory. This research has made use of the SIMBAD data base, operated at CDS, Strasbourg, France; the SAO/NASA Astrophysics Data System; and the VizieR catalogue access tool, CDS, Strasbourg, France. This research has made use of community-developed core PYTHON packages for astronomy (ASTROPY; Astropy Collaboration 2013, 2018), the PYTHON library for publication quality graphics (MATPLOTLIB; Hunter 2007), NUMPY (van der Walt, Colbert & Varoquaux 2011), and SCIPY (Virtanen et al. 2020).

Based on observations made with the Isaac Newton Telescope (INT) operated on the island of La Palma by the Isaac Newton Group (ING) in the Spanish Observatorio del Roque de los Muchachos of the Instituto de Astrofísica de Canarias.

DATA AVAILABILITY

The *Kepler* data underlying this article are available from the MAST archive (http://archive.stsci.edu/kepler/). All other data underlying this article will be shared on reasonable request to the corresponding author.

REFERENCES

Aerts C., 2021, Rev. Mod. Phys., 93, 015001
Aerts C., Christensen-Dalsgaard J., Kurtz D. W., 2010, Asteroseismology. Springer-Verlag, Berlin
Antoci V. et al., 2014, ApJ, 796, 118
Antoci V. et al., 2019, MNRAS, 490, 4040
Asplund M., Grevesse N., Sauval A. J., Scott P., 2009, ARA&A, 47, 481
Astropy Collaboration, 2013, A&A, 558, A33
Astropy Collaboration, 2018, AJ, 156, 123
Bailer-Jones C. A. L., Rybizki J., Fouesneau M., Mantelet G., Andrae R., 2018, AJ, 156, 58
Balona L. A., 2016, MNRAS, 459, 1097
Balona L. A., Dziembowski W. A., 2011, MNRAS, 417, 591
Balona L. A., Nemec J. M., 2012, MNRAS, 426, 2413
Balona L. A., Daszyńska-Daszkiewicz J., Pamyatnykh A. A., 2015, MNRAS, 452, 3073
Boonyarak C., Fu J.-N., Khokhuntod P., Jiang S.-Y., 2011, Ap&SS, 333, 125
Borucki W. J. et al., 2010, Science, 327, 977
Bowman D. M., 2016, PhD thesis, Jeremiah Horrocks Institute, University of Central Lancashire
Bowman D. M., 2017, Amplitude Modulation of Pulsation Modes in Delta Scuti Stars. Springer-Verlag, Berlin
Bowman D. M., Kurtz D. W., 2014, MNRAS, 444, 1909
Bowman D. M., Kurtz D. W., 2018, MNRAS, 476, 3169
Bowman D. M., Holdsworth D. L., Kurtz D. W., 2015, MNRAS, 449, 1004
Bowman D. M., Kurtz D. W., Breger M., Murphy S. J., Holdsworth D. L., 2016, MNRAS, 460, 1970
Breger M., 1990, in Cacciari C., Clementini G., eds, ASP Conf. Ser. Vol. 11, Confrontation Between Stellar Pulsation and Evolution. Astron. Soc. Pac., San Francisco, p. 263
Breger M., 2000a, in Szabados L., Kurtz D., eds, ASP Conf. Ser. Vol. 203, IAU Colloq. 176: The Impact of Large-Scale Surveys on Pulsating Star Research. Astron. Soc. Pac., San Francisco, p. 421
Breger M., 2000b, in Breger M., Montgomery M., eds, ASP Conf. Ser. Vol. 210, Delta Scuti and Related Stars. Astron. Soc. Pac., San Francisco, p. 3
Breger M., 2000c, MNRAS, 313, 129
Breger M., Montgomery M. H., 2014, ApJ, 783, 89
Breger M., Pamyatnykh A. A., 1998, A&A, 332, 958
Breger M. et al., 2011, MNRAS, 414, 1721
Breger M. et al., 1993, A&A, 271, 482
Brickhill A. J., 1992, MNRAS, 259, 519
Brown T. M., Latham D. W., Everett M. E., Esquerdo G. A., 2011, AJ, 142, 112
Butters O. W. et al., 2010, A&A, 520, L10
Coates D. W., Halprin L., Thompson K., 1982, MNRAS, 199, 135
Currie M. J., Berry D. S., Jenness T., Gibb A. G., Bell G. S., Draper P. W., 2014, in Manset N., Forshay P., eds, ASP Conf. Ser. Vol. 485, Astronomical Data Analysis Software and Systems XXIII. Astron. Soc. Pac., San Francisco, p. 391
Daszyńska-Daszkiewicz J., Pamyatnykh A. A., Walczak P., Szewczuk W., 2020, MNRAS, 499, 3034
Degroote P. et al., 2009, A&A, 506, 111
Derekas A. et al., 2009, MNRAS, 394, 995
Dotter A., 2016, ApJS, 222, 8
Dupret M. A., Grigahcène A., Garrido R., Gabriel M., Scuflaire R., 2005, A&A, 435, 927
Dziembowski W., 1977, Acta Astron., 27, 95
Dziembowski W., Krolikowska M., 1985, Acta Astron., 35, 5
Dziembowski W. A., Pamyatnykh A. A., 2008, MNRAS, 385, 2061
Evans D. F., 2018, Res. Notes Am. Astron. Soc., 2, 20
Frolov M. S., Irkaev B. N., 1984, Information Bulletin on Variable Stars, 2462
Gaia Collaboration, 2016, A&A, 595, A1

Gaia Collaboration, 2018, A&A, 616, A1
Gaia Collaboration, 2021, A&A, 649, A1
Goodricke J., 1783, Phil. Trans. R. Soc., 73, 474
Gray D. F., 2005, The Observation and Analysis of Stellar Photospheres, 3rd edn. Cambridge Univ. Press, Cambridge
Gray R. O., Corbally J. C., 2009, Stellar Spectral Classification. Princeton Univ. Press, Princeton, NJ
Green G. M. et al., 2018, MNRAS, 478, 651
Guzik J. A., Cox A. N., 1991, Delta Scuti Star Newsletter, 3, 6
Hermans J., 2019, Master's thesis, Institute of Astronomy
Heynderickx D., Waelkens C., Smeyers P., 1994, A&AS, 105, 447
Holdsworth D. L., 2015, PhD thesis, Keele University
Huber D. et al., 2014, ApJS, 211, 2
Hunter J. D., 2007, Comput. Sci. Eng., 9, 90
Iben I. Jr, 1967, ARA&A, 5, 571
Iglesias C. A., Rogers F. J., 1996, ApJ, 464, 943
Jayasinghe T. et al., 2020, MNRAS, 493, 4186
Kippenhahn R., Weigert A., Weiss A., 2012, Stellar Structure and Evolution. Springer-Verlag, Berlin
Kjeldsen H., Bedding T. R., 1995, A&A, 293, 87
Kurtz D. W., 1985, MNRAS, 213, 773
Kurtz D. W., Shibahashi H., Murphy S. J., Bedding T. R., Bowman D. M., 2015, MNRAS, 450, 3015
Lares-Martiz M., Garrido R., Pascual-Granado J., 2020, MNRAS, 498, 1194
Lee Y.-H., Kim S. S., Shin J., Lee J., Jin H., 2008, PASJ, 60, 551
Loumos G. L., Deeming T. J., 1978, Ap&SS, 56, 285
McNamara D., 1997, PASP, 109, 1221
McNamara D. H., 2000a, PASP, 112, 1096
McNamara D. H., 2000b, in Breger M., Montgomery M., eds, ASP Conf. Ser. Vol. 210, Delta Scuti and Related Stars. Astron. Soc. Pac., San Francisco, p. 373
McNamara D. H., 2011, AJ, 142, 110
Maeder A., 2009, Physics, Formation and Evolution of Rotating Stars. Springer-Verlag, Berlin
Maeder A., Meynet G., 2000, ARA&A, 38, 143
Mathur S. et al., 2017, ApJS, 229, 30
Moskalik P., 1985, Acta Astronomica, 35, 229
Murphy S. J., 2014, PhD thesis, Jeremiah Horrocks Institute, University of Central Lancashire
Murphy S. J., Shibahashi H., Kurtz D. W., 2013a, MNRAS, 430, 2986
Murphy S. J. et al., 2013b, MNRAS, 432, 2284
Murphy S. J., Hey D., Van Reeth T., Bedding T. R., 2019, MNRAS, 485, 2380
Murphy S. J., Saio H., Takada-Hidai M., Kurtz D. W., Shibahashi H., Takata M., Hey D. R., 2020, MNRAS, 498, 4272
Nemec J. M., Balona L. A., Murphy S. J., Kinemuchi K., Jeon Y.-B., 2017, MNRAS, 466, 1290
Niemczura E. et al., 2015, MNRAS, 450, 2764
Pamyatnykh A. A., 1999, AcA, 49, 119
Pamyatnykh A. A., 2000, in Breger M., Montgomery M., eds, ASP Conf. Ser. Vol. 210, Delta Scuti and Related Stars. Astron. Soc. Pac., San Francisco, p. 215
Pamyatnykh A. A., Dziembowski W. A., Handler G., Pikall H., 1998, A&A, 333, 141
Pápics P. I., 2012, Astron. Nachr., 333, 1053
Pápics P. I. et al., 2012, A&A, 542, A55
Percy J. R., Matthews J. M., Wade J. D., 1980, A&A, 82, 172
Petersen J. O., 1973, A&A, 27, 89
Petersen J. O., Christensen-Dalsgaard J., 1996, A&A, 312, 463
Pigulski A., Pojmański G., Pilecki B., Szczygieł D. M., 2009, AcA, 59, 33
Poleski R. et al., 2010, AcA, 60, 1
Pollacco D. L. et al., 2006, PASP, 118, 1407
Poretti E., 2003, A&A, 409, 1031
Ricker G. R. et al., 2015, J. Astron. Telesc. Instrum. Syst., 1, 014003
Rizzuto A. C., Vanderburg A., Mann A. W., Kraus A. L., Dressing C. D., Agüeros M. A., Douglas S. T., Krolikowski D. M., 2018, AJ, 156, 195
Rodríguez E., Breger M., 2001, A&A, 366, 178
Rodríguez E., López de Coca P., Costa V., Martín S., 1995, A&A, 299, 108
Rodríguez E., López-González M. J., López de Coca P., 2000, A&AS, 144, 469
Rodríguez E. et al., 2007, A&A, 471, 255
Shulyak D., Tsymbal V., Ryabchikova T., Stütz C., Weiss W. W., 2004, A&A, 428, 993
Smalley B., 1993, A&A, 274, 391
Smalley B., 2005, Mem. Soc. Astron. Ital. Suppl., 8, 130
Smith J. C. et al., 2012, PASP, 124, 1000
Soszyński I. et al., 2008, Acta Astron., 58, 163
Stellingwerf R. F., 1978, AJ, 83, 1184
Stellingwerf R. F., 1979, ApJ, 227, 935
Sterken C., 2005, in Sterken C., ed., ASP Conf. Ser. Vol. 335, The Light-Time Effect in Astrophysics: Causes and cures of the O-C diagram. Astron. Soc. Pac., San Francisco, p. 3
Stumpe M. C. et al., 2012, PASP, 124, 985
Tamuz O., Mazeh T., Zucker S., 2005, MNRAS, 356, 1466
Thompson K., Coates D. W., 1991, Proc. Astron. Soc. Aust., 9, 281
Tkachenko A., 2015, A&A, 581, A129
Tkachenko A., Lehmann H., Smalley B., Uytterhoeven K., 2013, MNRAS, 431, 3685
Tsymbal V., 1996, in Adelman S. J., Kupka F., Weiss W. W., eds, ASP Conf. Ser. Vol. 108, M.A.S.S., Model Atmospheres and Spectrum Synthesis. Astron. Soc. Pac., San Francisco, p. 198
Uytterhoeven K. et al., 2011, A&A, 534, A125
van der Walt S., Colbert S. C., Varoquaux G., 2011, Comput. Sci. Eng., 13, 22
Van Reeth T. et al., 2015, A&A, 574, A17
Virtanen P. et al., 2020, Nat. Methods, 17, 261
Walraven T., Walraven J., Balona L. A., 1992, MNRAS, 254, 59
Watson R. D., 1988, Ap&SS, 140, 255
Yang T. et al., 2018, ApJ, 863, 195
Yang X. H., Fu J. N., Zha Q., 2012, AJ, 144, 92
Ziaali E., Bedding T. R., Murphy S. J., Van Reeth T., Hey D. R., 2019, MNRAS, 486, 4348
Zorec J., Royer F., 2012, A&A, 537, A120

APPENDIX: FREQUENCY LISTS

The additional independent non-radial pulsation mode frequencies identified in the LC and SC *Kepler* data of KIC 5950759 are provided in Tables A1 and A2, respectively.

Table A1. Additional independent frequencies extracted from the 4-yr LC *Kepler* data of KIC 5950759 (i.e. after ν_1 and ν_2 and all their significant harmonics and combinations have been removed). Pulsation phases were calculated with respect to the time zero-point $t_0 = 2455688.770$ BJD (i.e. the midpoint of the 4-yr LC light curve).

Frequency (d^{-1})	Amplitude (mmag)	Phase (rad)
0.31925 ± 0.00004	0.284 ± 0.030	1.99 ± 0.11
16.00000 ± 0.00006	0.202 ± 0.030	2.03 ± 0.15
18.45070 ± 0.00009	0.125 ± 0.030	−0.17 ± 0.24
18.96828 ± 0.00008	0.149 ± 0.030	1.47 ± 0.20
20.34427 ± 0.00005	0.229 ± 0.030	2.24 ± 0.13
21.15701 ± 0.00005	0.211 ± 0.030	2.25 ± 0.14
21.49656 ± 0.00004	0.291 ± 0.030	1.69 ± 0.10
22.62858 ± 0.00003	0.442 ± 0.030	−2.44 ± 0.07
23.70270 ± 0.00006	0.187 ± 0.030	−0.97 ± 0.16
23.82188 ± 0.00006	0.192 ± 0.030	0.06 ± 0.16
24.67230 ± 0.00003	0.380 ± 0.030	−1.32 ± 0.08
25.36702 ± 0.00004	0.295 ± 0.030	−1.57 ± 0.10

Table A2. Additional independent frequencies extracted from the residual 31-d SC *Kepler* data of KIC 5950759 (i.e. after ν_1 and ν_2 and all their significant harmonics and combinations have been removed). Pulsation phases were calculated with respect to the time zero-point $t_0 = 2455200.895$ BJD (i.e. the midpoint of the 31-d SC light curve).

Frequency (d^{-1})	Amplitude (mmag)	Phase (rad)
15.9977 ± 0.0019	0.42 ± 0.05	1.46 ± 0.11
18.4513 ± 0.0018	0.47 ± 0.05	1.63 ± 0.10
18.9699 ± 0.0018	0.45 ± 0.05	0.91 ± 0.10
20.3421 ± 0.0014	0.58 ± 0.05	-0.62 ± 0.08
21.1629 ± 0.0017	0.48 ± 0.05	1.95 ± 0.10
21.4957 ± 0.0007	1.19 ± 0.05	-2.47 ± 0.04
22.6277 ± 0.0012	0.69 ± 0.05	-2.24 ± 0.07
23.7050 ± 0.0021	0.39 ± 0.05	-1.18 ± 0.12
23.8250 ± 0.0012	0.71 ± 0.05	-0.84 ± 0.06
24.6676 ± 0.0009	0.88 ± 0.05	-1.03 ± 0.05
25.3680 ± 0.0016	0.51 ± 0.05	-0.75 ± 0.09
28.3737 ± 0.0015	0.56 ± 0.05	0.57 ± 0.08
33.6469 ± 0.0013	0.64 ± 0.05	2.83 ± 0.07

This paper has been typeset from a TEX/LATEX file prepared by the author.